International Journal of Biological Macromolecules 54 (2013) 109–118

Contents lists available at SciVerse ScienceDirect

International Journal of Biological Macromolecules

journal homepage: www.elsevier.com/locate/ijbiomac

Thermal denaturation and aggregation of hemoglobin of *Glossoscolex paulistus* in acid and neutral media

José Wilson P. Carvalho[a], Francisco A.O. Carvalho[a], Patrícia S. Santiago[a,b], Marcel Tabak[a,*]

[a] *Instituto de Química de São Carlos, Universidade de São Paulo, Av. Trabalhador Sancarlense, 400, 13560-970 São Carlos, SP, Brazil*
[b] *Universidade Estadual Paulista "Julio de Mesquita Filho", Registro, São Paulo, SP, Brazil*

ARTICLE INFO

Article history:
Received 22 October 2012
Received in revised form
16 November 2012
Accepted 20 November 2012
Available online 26 November 2012

Keywords:
Extracellular hemoglobin
Glossoscolex paulistus
Denaturation and aggregation
DSC
AUC
DLS

ABSTRACT

The thermal denaturation and aggregation of the HbGp, in the oxy- and cyanomet-forms, was investigated by DSC, AUC, DLS, optical absorption and CD, in the pH range from 5.0 to 7.0. Oxy-HbGp has a denaturation process partially reversible and dependent on the temperature. DSC melting curve is characterized by a single peak with T_c value of 333.4 ± 0.2 K for oxy-HbGp, while two peaks with T_c values of 332.2 ± 0.1 and 338.4 ± 0.2 K are observed for cyanomet-HbGp, at pH 7.0. In acidic pH oxy- and cyanomet-HbGp are more stable showing higher T_c values and aggregation. AUC data show that, HbGp, at pH 7.0, upon denaturation, remains undissociated at 323 K, presenting oligomeric dissociation at 333 (12 ± 3% of tetramer and 88 ± 5% of whole HbGp) and 343 K (70 ± 5% of monomer and 30 ± 2% of trimer). DLS data show that the lag period before aggregation is dependent on the temperature and HbGp concentration. Optical absorption and CD results show that the increase of temperature leads to the oxy-HbGp oxidation and aggregation, above 331 K, in acidic pH. CD data, for HbGp, present a greater thermal stability in acid medium than at neutral pH, with similar T_c values for both oxidation forms. Our data are consistent with previous studies and represents an advance in understanding the thermal stability of oligomeric HbGp structure.

1. Introduction

The giant extracellular hemoglobin of *Glossoscolex paulistus* (HbGp) has a complex oligomeric structure, composed of heme-containing globin-like subunits forming a tetramer, ***abcd***, and additional subunits lacking a heme group, and named linkers. A total molecular mass of 3.6×10^6 Da, similar to that of other extracellular hemoglobins, has been reported in recent years [1–5].

HbGp is orthologous to the hemoglobin of *Lumbricus terrestris* (HbLt), and recent partial characterization of the molecular masses of HbGp subunits [6,7] confirmed its similarity to the orthologous proteins of this class [1–3,8]. The similarity between HbGp and HbLt is based on spectroscopic and hydrodynamic studies [5–11]. Moreover, a recent preliminary study of HbGp crystallographic structure, at 3.2 Å resolution, indicates that the hierarchical levels of HbGp organization are very similar to HbLt [12]. Due to its extracellular nature, large size and resistance to oxidation, giant extracellular hemoglobins, also known as erythrocruorins, have been proposed as useful model systems for developing therapeutic extracellular blood substitutes [2–4,8]. Since cell membranes are not present and the protein is not glycosilated, hexagonal bilayer hemoglobins are easy to store, their side effects are less pronounced, and they are less likely to trigger immunogenic responses [3,4,8].

In a previous work, the thermal stability of HbGp has been investigated, and results were reported, based on dynamic light scattering (DLS), showing that oxy-HbGp is stable up to 325 K, at pH 7.0 [13]. At higher temperatures, oxy-HbGp denatured and formed aggregates. In acid solution, HbGp is also very stable, undergoing denaturation with a strong aggregation and formation of large aggregates, near to the isoelectric point (pI ∼ 5.5 [14]). On the other hand, in the alkaline pH range, increase of temperature leads to the oligomeric dissociation of oxy-HbGp, at temperatures 317–305 K, in the pH range from 7.5 to 8.3, followed by denaturation at higher temperatures [13]. More recently, thermal denaturation studies were reported for oxy- and cyanomet-HbGp, based on differential scanning calorimetry (DSC [15]). For the first time thermodynamic parameters for HbGp, at pH values 7.0 and 8.0, were obtained [15]. Cyanomet-HbGp was shown to be more stable than the oxy-HbGp, and both protein oxidation forms have high activation energies, at pH 7.0 and 8.0. In agreement with DLS data, studies based on the DSC technique show that the oxy-HbGp, at alkaline pH, undergoes oligomeric dissociation before denaturation. Furthermore, HbGp thermal denaturation process is dependent on the protein concentration, the critical denaturation temperature increasing with protein concentration [15].

* Corresponding author. Fax: +55 16 33739982.
E-mail address: marcel@sc.usp.br (M. Tabak).

0141-8130
http://dx.doi.org/10.1016/j.ijbiomac.2012.11.022

In this paper, further studies were performed with oxy- and cyanomet-HbGp, aiming to obtain the thermodynamic parameters related to the denaturation process, as monitored by optical absorption spectroscopy, circular dichroism (CD), and DSC. The experimental data were analyzed based on the fits with the two-state model, widely used in interpretation of protein denaturation data analyses [16–19]. Additionally, we focus in the kinetic studies of thermal aggregation of HbGp, at different protein concentrations, and fixed pH 7.0, in the temperature range from 323 to 327 K. Our present results contribute to further understanding of the thermal stability of this complex oligomeric protein.

2. Materials and methods

2.1. Preparation of the oxy- and cyanomet-HbGp forms

HbGp was prepared using freshly drawn blood from worms as described earlier [10–15]. The blood sample was centrifuged at 4 °C (2300 × *g* for 15 min) to eliminate cell debris. An ultra-filtration (molecular mass cut-off 30 kDa) in 0.1 mol/L Tris–HCl buffer pH 7.0, at 4 °C, was performed in order to eliminate low molecular weight components. After the ultracentrifugation at 250,000 × *g*, at 4 °C, for 3 h, HbGp is obtained as a pellet, and then re-suspended in a minimum volume of 0.1 mol/L Tris–HCl buffer, at pH 7.0, and stored in the oxy-form at 4 °C. Chromatography at pH 7.0 in a Sephadex G-200 column gave the pure samples used in our experiments. All concentrations were determined spectrophotometrically in a UV-1601 PC spectrophotometer (Shimadzu, Japan), using the extinction coefficients $\varepsilon_{415} = 5.5 \pm 0.8\,(\text{mg/mL})^{-1}\,\text{cm}^{-1}$ for oxy-HbGp, and $\varepsilon_{420} = 4.8 \pm 0.5\,(\text{mg/mL})^{-1}\,\text{cm}^{-1}$ for cyanomet-HbGp [14,15].

2.2. Differential scanning calorimetry (DSC)

DSC experiments were performed for oxy- and cyanomet-HbGp forms, at a protein concentration of 0.5 mg/mL, in phosphate 30 mmol/L buffer, in the pH range from 5.0 to 7.0. The measurements were made in a VP-DSC Microcal (Northampton, MA) instrument. The runs were made in the temperature range from 298 to 363 K, keeping the sample under a pressure of 2 atm, and using a heating rate of 1 K min^{-1}. All samples were stabilized for 15 min at the initial temperature, before starting the heating cycle. A sequence of heating cycles was performed in the same sample in order to evaluate the reversibility of the HbGp thermal denaturation process, at pH 7.0. Buffer versus buffer baseline scans were determined and subtracted from the sample scans to perform the analysis of protein denaturation.

DSC data analyses were performed based on the model proposed by Sanchez-Ruiz [16,17], using the Microcal *Origin 7.0* software. Two and three-state denaturation models were used in the data fittings and thermodynamic parameters, such as the critical temperature (T_c) and apparent calorimetric enthalpy (ΔH_{app}), corresponding to the midpoint of the fitted endotherm curve was obtained. In this paper the symbol T_c is used along the text rather than the melting temperature T_m, commonly used in many calorimetric studies. The meaning of this parameter is essentially the same, independent of the monitoring method, either by optical spectroscopy or DSC.

2.3. Dynamic light scattering (DLS)

The instrument Zetasizer Nano ZS (Malvern, UK) was used for the light scattering measurements and particle size determination. This instrument allows dynamic light scattering measurements incorporating noninvasive backscattering (NIBS) optics. A He–Ne laser has been used as a light source with wavelength λ = 633 nm. The intensity of light scattered at an angle of 173° is measured by an avalanche photodiode. The solutions were placed in the thermostated sample chamber that maintained the sample stabilized, with an accuracy of 0.1 K. The kinetic thermal aggregation experiments were performed using oxy-HbGp in the concentrations of 0.5, 1.0 and 3.0 mg/mL, at pH 7.0, in the phosphate 30 mmol/L buffer, in the temperature range from 323 to 327 K. Samples were prepared following identical procedures as those used for DSC studies.

The thermal aggregation process for HbGp monitoring the hydrodynamic diameter by DLS was analyzed estimating the lag period (t_0) using the following equation [20]:

$$D_h = D^*_{h,0}\left(1 + \frac{(t - t_0)}{t_{2D}}\right) \quad (1)$$

where $D^*_{h,0}$ corresponds to the hydrodynamic diameter of the protein at the initial time of the aggregation process, t_0 is the duration of the lag period before the aggregation process, and t_{2D} is the time necessary for the D_h value to be doubled [20]. Calculations were made with Microcal *Origin 8.0* program.

2.4. Analytical ultracentrifugation (AUC)

Samples of oxy-HbGp, 3.0 mg/mL, were subjected to heating, maintaining them at 323, 333 and 343 K for 1 h, with subsequent cooling down to room temperature (298 K). After this heating treatment, all samples were centrifuged at 5000 rpm, collecting the supernatant for absorption spectral analysis, in the range between 250 and 700 nm. The amount of protein remaining in solution was estimated based on the absorbance values at 415 nm.

The AUC measurements were made with protein concentrations of 100, 200 and 300 μg/mL, in 100 mmol/L phosphate buffer pH 7.0, containing 50 mmol/L NaCl. A Beckman Optima XL-A analytical ultracentrifuge was used and sedimentation velocity (SV) experiments were performed at 20 °C, using a rotor speed between 15,000 and 40,000 rpm (An-60Ti rotor), with acquisition of scan data at 414 nm. A radial step size of 0.003 cm was used for collection of absorbance data.

The sedimentation coefficient values contain interferences caused by temperature, viscosity (η) and density (ρ), so the standard sedimentation coefficient at infinite dilution (0 mg/mL, $s^0_{20,w}$) was calculated. The Sednterp software was used to estimate the η and ρ values for protein solution in buffer [21,22]. AUC data were analyzed using SEDFIT (version 13.0 [22–24]) and SEDPHAT (version 10.4 [24]) software, as described elsewhere [5,25].

The analyses of the molecular masses (*MM*) of the HbGp subunits, present in solution, in the SV experiments, were performed from the global fitting with the "Species Analysis" model of the SEDPHAT program [24]. SV data for oxy-HbGp, at three different concentrations, were analyzed by global fits using SEDPHAT program. All parameters were allowed to float freely, and statistical analyses were performed, based on the "Monte-Carlo non-linear regression" with 300 iterations and a confidence level of 0.68.

2.5. Spectroscopic measurements

Optical absorption spectra, in the range between 700 and 250 nm, were measured in a UV-1601 PC spectrophotometer (Shimadzu, Japan) equipped with a temperature controller (Peltier, TCC-Controller operating in the range from 283 to 343 K). The oxy- and cyanomet-HbGp forms were analyzed at a protein concentration of 0.2 mg/mL, in phosphate 30 mmol/L solutions, varying the pH in the range 5.0–7.0. The optical absorption spectra were obtained in the temperature range between 293 and 343 K, at 2 K interval, and an equilibrium time of six minutes at each temperature.

Circular dichroism (CD) measurements were carried out using the Jasco J-810 spectropolarimeter (JASCO, Japan). The CD spectra were obtained for two different spectral regions corresponding to the peptide bonds (190–250 nm) and heme groups and aromatic amino acids (250–500 nm), with 1 mm path length cell [26,27]. Scan speeds of 100 and 200 nm/min were used, respectively, in the two regions. A spectral resolution of 0.5 nm, and an average of eight scans were used. The samples were prepared following similar procedures as described for optical absorption measurements above, in the pH range from 5.0 to 7.0, in phosphate 30 mmol/L, and at protein concentrations of 0.2 and 3.0 mg/mL, for the peptide bonds and the heme regions, respectively, for the oxy- and cyanomet-HbGp forms.

Data analysis to obtain the critical denaturation temperature was performed under the assumption of a two-state denaturation model [17–19]. The apparent enthalpy (ΔH_{app}) and critical temperature (T_c) values may be estimated using Eq. (2):

$$y = \left(\frac{(y_F + m_F \cdot T) + (y_U + m_U \cdot T)\exp(\Delta H((T/T_c) - 1) + \Delta C_p(T_c - T + T \cdot \ln(T/T_c)))/RT}{1 + \exp((\Delta H(T/T_c) - 1) + \Delta C_p(T_c - T + T \cdot \ln(T/T_c))/RT)} \right) \quad (2)$$

where y is the measured signal at a given temperature, higher than the initial one, y_F and y_U are the intercepts, and m_F and m_U are the slopes of the pre- (folded state) and post-transition (unfolded state) baselines, T is the temperature, T_c is the midpoint of the thermal unfolding curve, and ΔH_{app} is the apparent enthalpy change for protein unfolding at T_c [19].

3. Results and discussion

3.1. DSC thermal stability analysis for oxy- and cyanomet-HbGp

Fig. 1 shows the melting curves obtained by DSC for oxy-HbGp, at a concentration of 0.5 mg/mL, at pH 7.0. Scan x corresponds to the first heating cycle, and the scan x′ to the re-heating of the same sample (Fig. 1A). The first scan is characterized by a single peak with a critical temperature (T_c) of 333 K, while the second scan does not show any peak, indicating that the HbGp has an irreversible denaturation process (Fig. 1A). In addition, the reversibility of the thermal denaturation was assayed, through multiple DSC heating scans with a scan rate of 1 K min^{-1} to evaluate the temperatures corresponding to complete or partial irreversible thermal denaturation for oxy-HbGp. Fig. 1B shows these sequential heating cycles of the sample. The first one was up to 331 K (scan a), corresponding to 2 K less than the critical temperature (Fig. 1B). The reversibility is 100% in this case. Then, the sample is cooled back to the starting temperature and a second heating cycle is performed up to 333 K (scan b), corresponding to the critical temperature, when the denaturation of HbGp is observed (Fig. 1B). The scan b shows also a reversibility degree around 64 ± 5% (Fig. 1B). The next cycle corresponds to heating of the sample to a temperature 1 K higher than the critical one, and, finally, heating up to 365 K does not show any peak, in agreement with the irreversible denaturation of HbGp.

This experiment indicates that the irreversible denaturation of HbGp is caused by the high temperature, and heating of the sample up to T_c is enough to achieve the complete protein denaturation irreversibility. Moreover, these results suggest that the HbGp denaturation process follows the Lumry–Eyring model [16,28]. This model is described by two different steps. The first process involves a reversible step, followed by an irreversible process, as shown by the following equation:

$$N \underset{k_{-1}}{\overset{k_1}{\rightleftarrows}} U \xrightarrow{k_2} F \quad (3)$$

where in this case N, U and F are native, unfolded and final irreversible denatured states of the protein, and k_1, k_{-1} and k_2 are the rate constants for each step. The U state is a reversibly unfolded state of the native protein N. According to the Lumry–Eyring model k_2 is significantly higher than k_{-1} ($k_2 \gg k_{-1}$), so that most of the molecules in the U state are converted to the F state, resulting in the lack of refolding back into the native protein form. The denaturation process can be expressed also as a single-step process following first-order kinetics, as shown in Eq. (4) [15,16,28]:

$$N \xrightarrow{k} F \quad (4)$$

this model is widely used for the treatment of irreversible processes monitored by DSC measurements. It has been used for the interpretation of DSC data obtained for hemocyanins [29–32]. In our case, the irreversible denaturation process for oligomeric oxy-HbGp can be analyzed, based on the two-state model described above and developed by Sanchez-Ruiz [16]. This interpretation provides a good analysis of our DSC data, as well as, a consistent description of the results based on the several other techniques discussed later in this paper.

Additional DSC studies were performed with oxy- and cyanomet-HbGp, in neutral and acid pH solutions, as shown in Fig. 2. Furthermore, based on the model developed by Sanchez-Ruiz [16] the DSC melting endotherms were analyzed (Fig. 2A and B). Oxy-HbGp presents a single quite cooperative endothermic transition (Fig. 2A), while cyanomet-HbGp (Fig. 2B) displays,

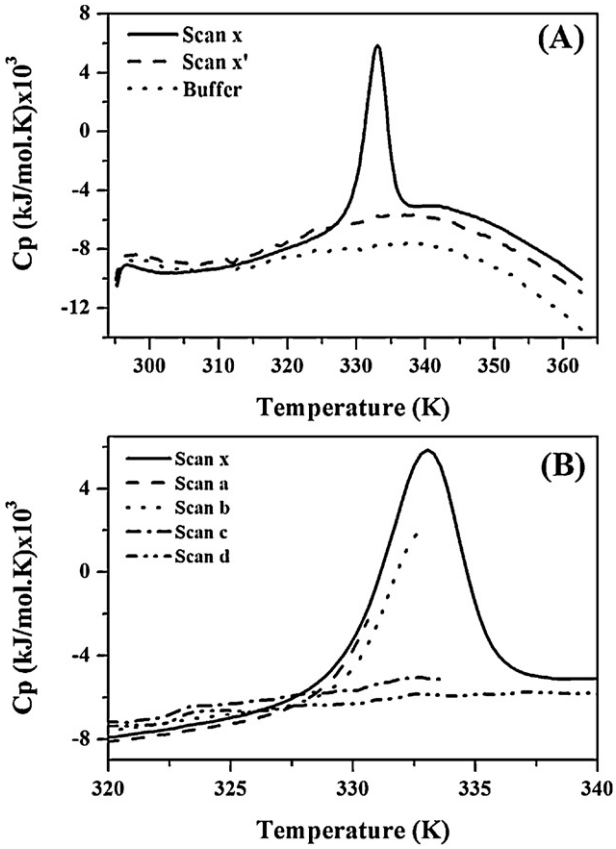

Fig. 1. Experimental DSC thermograms for oxy-HbGp 0.5 mg/mL, in phosphate buffer 30 mmol/L, at pH 7.0, in the temperature range from 292 to 365 K, and a scan rate of 1.0 K min^{-1}. (A) Scan x corresponds to a full scan up to 365 K; scan x′ corresponds to a second consecutive scan after cooling back the sample to the initial temperature of 292 K. (B) Consecutive scans of the same sample up to the following temperatures: 331 K (a), 333 K (b), 334 K (c) and 365 (d).

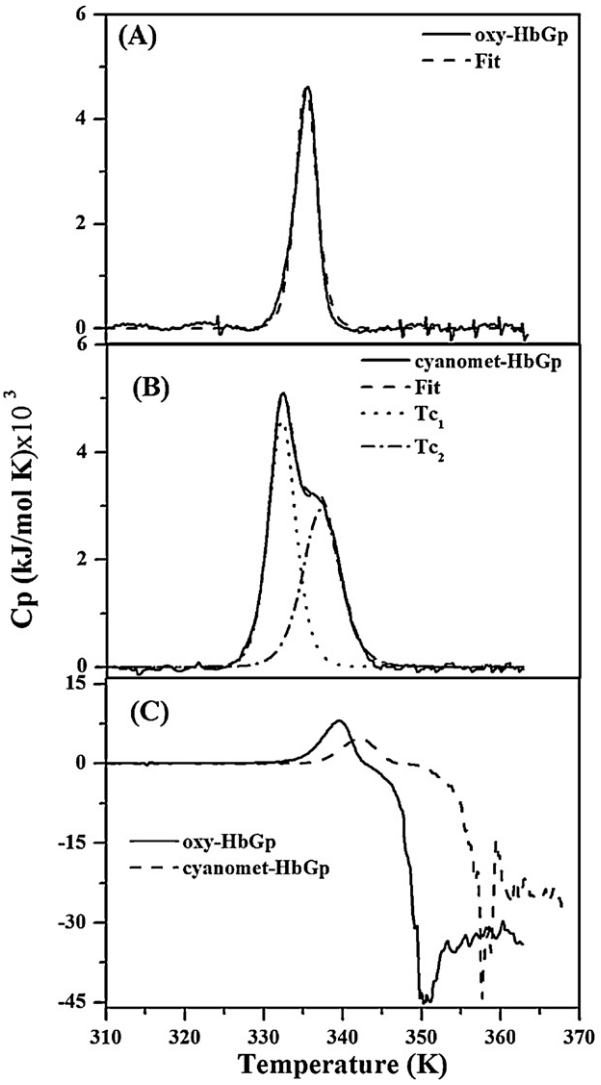

Fig. 2. DSC thermograms for oxy- and cyanomet-HbGp 0.5 mg/mL, in phosphate-acetate buffer 30 mmol/L, at a scan rate of 1.0 K min^{-1}. (A) Oxy-HbGp, at pH 7.0. (B) Cyanomet-HbGp, at pH 7.0. (C) Oxy- and cyanomet-HbGp, at pH 5.0.

clearly, two transitions that compose the whole endotherm, without any evidence of an exothermic peak associated to protein aggregation [33,34]. At pH 5.0, both HbGp forms present endothermic transitions shifted to higher temperatures together with an exothermic process, at elevated temperatures, above 343 K, in the range between 348 and 361 K, associated to protein aggregation (Fig. 2C).

As seen in Fig. 2A, a single component fit using a simple two-state model was adequate to describe the oxy-HbGp endotherm. On the other hand, for the cyanomet-HbGp the best fit was obtained using two components (Fig. 2B). The critical temperatures (T_c) obtained from the fits, the individual calorimetric apparent enthalpies (ΔH_{app}) and the total transition enthalpies, are displayed in Table 1. The T_c values for cyanomet-HbGp are systematically higher as compared to oxy-HbGp. T_c values, at pH 7.0, are 333.4 ± 0.2 K, for oxy-HbGp (one component), and 332.2 ± 0.1 K and 338.4 ± 0.2 K (two components) for cyanomet-HbGp (Table 1). It is possible that, for cyanomet-HbGp, the temperature-induced oligomeric dissociation and the denaturation occur relatively slower as compared to the oxy-form, allowing the partial resolution of the two processes of dissociation and denaturation.

For oxy-HbGp, the temperature-induced oligomeric dissociation process occurs faster leading to a single denaturation temperature for all domains, as compared to cyanomet-HbGp (Fig. 2A and B). This difference in stability between the domains of cyanomet-HbGp may be due to the contribution of the cyanide (CN^-) ligand in the sixth iron coordination position. Since the stability of cyanomet-HbGp is higher, in this case the thermal denaturation process of HbGp can be altered and several components are observed in the oligomeric dissociation into isolated subunits.

In Fig. 2C the endotherms for oxy- and cyanomet-HbGp, at pH 5.0, are shown. The HbGp denaturation endotherms, shown in Fig. 2C, are not simple two-state transitions, since it was not possible to obtain their adequate fits using the simple two-state model. In order to obtain a proper fit for the experimental endotherms, two components were necessary, for both oxy- and cyanomet-HbGp (Table 1), at pH values 5.0 (see Fig. S1 in the Supplementary data), and 6.0 (not shown), suggesting similar denaturation/aggregation processes for both oxidation forms of HbGp. T_c values for cyanomet-HbGp are systematically higher, as compared to oxy-HbGp: at pH 5.0, the T_c values for the two components are 338.3 ± 0.1 and 340.2 ± 0.2 K, for oxy-, and 341.3 ± 0.2 and 343.1 ± 0.2 K, for cyanomet-HbGp (see Table 1). At pH 6.0 (data not shown), oxy- and cyanomet-HbGp show a very similar behavior as for pH 5.0 (Table 1).

In this context, the results obtained for another protein of this class, *Rapana thomasiana* hemocyanin [32], presenting a complex thermal denaturation process, monitored by DSC, with an endotherm composed of several transitions, as observed for HbGp and *Concholepas concholepas* hemocyanin (CCH [31]), are worthy of notice. The best fit of the complex endotherm for *Rapana thomasiana* was made using several components, rationalized as associated to the denaturation of different subunits, constituting the whole oligomeric structure. Comparison of HbGp thermal denaturation with those observed for other proteins, as, for example, CCH hemocyanin [31], is worthwhile since it also presents a complex oligomeric structure. The denaturation process in hemocyanins, at several experimental conditions, is also an irreversible process, characterized by kinetic control, and protein concentration dependence. A broad endotherm is also observed, which cannot be described by a single two-state transition, but, instead, can be well fitted by a sum of, at least, three transitions, with T_c values higher than 81 °C. In addition, different domains of CCH, composing the oligomeric structure, undergo denaturation in a more or less independent way, justifying the broad endotherm with several transitions, associated with different components [31].

3.2. Thermal denaturation of HbGp evaluated by analytical ultracentrifugation

In order to evaluate in more detail the HbGp oligomeric dissociation induced by the temperature increase, AUC experiments with the oxy-HbGp, at pH 7.0, and submitted to heating at the temperatures of 323, 333 and 343 K, were performed (see Section 2.4 for details and [5,25]). In Fig. 3 the continuous sedimentation coefficient distributions, c(S), for oxy-HbGp, at pH 7.0, are shown. The corresponding hydrodynamic parameters are displayed in Table 2. At 323 K (Fig. 3, closed squares) only a single species is observed in solution, with $s^0_{20,w}$ of 57 ± 1 S and *MM* at 3530 ± 50 kDa, corresponding to the undissociated HbGp [5]. Thus, the protein is maintained in its native form in solution, at 323 K. On the other hand, pre-heating of oxy-HbGp, at 333 K, leads to the appearance of two contributions in the c(S) curve (Fig. 3, open triangles). The first one, with a relative percentage of 12%, and a $s^0_{20,w}$ of 4.2 ± 0.3 S and *MM* of 67.1 ± 0.2 kDa, is associated to the tetramer subunit (***abcd***, Table 2). The second one, with a contribution of 88 ± 5%, corresponds to the whole HbGp. Moreover, the formation of

Table 1
Critical temperatures (T_c) and apparent calorimetric enthalpy (ΔH_{app}) values for HbGp, in the oxy- and cyanomet-forms, at a protein concentration of 0.5 mg/mL, obtained from DSC experiments, at a heating rate of 1.0 K min^{-1}, at indicated pH values from 5.0 to 7.0.

	pH	T_{c1} (K)	$\Delta H_{app\ 1}$ (MJ/mol)	T_{c2} (K)	$\Delta H_{app\ 2}$ (MJ/mol)	$\Delta H_{app\ total}$ (MJ/mol)
Oxy-HbGp	5.0	338.3 ± 0.1	27 ± 7	340.2 ± 0.2	20 ± 8	47 ± 15
	6.0	339.2 ± 0.1	30 ± 7	341.1 ± 0.1	21 ± 7	51 ± 14
	7.0	333.4 ± 0.2	33 ± 3	–	–	33 ± 3
Cyanomet-HbGp	5.0	341.3 ± 0.2	26 ± 8	343.1 ± 0.2	16 ± 8	44 ± 16
	6.0	340.1 ± 0.1	27 ± 3	342.3 ± 0.1	31 ± 3	58 ± 6
	7.0	332.2 ± 0.1	30 ± 3	338.4 ± 0.2	20 ± 2	50 ± 5

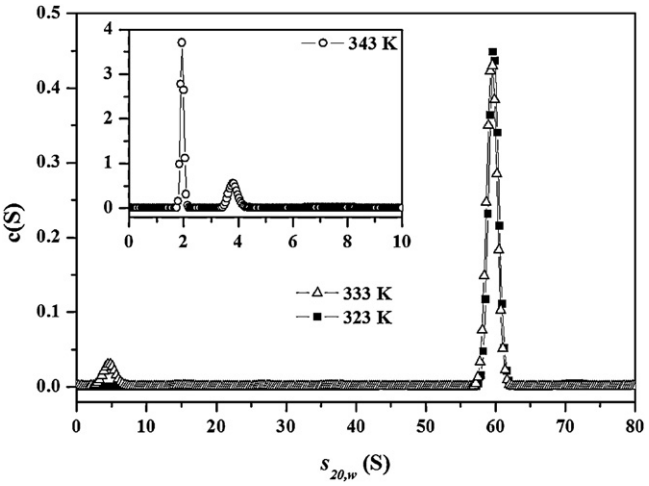

Fig. 3. Continuous sedimentation coefficient distributions, c(S), for oxy-HbGp 300 μg/mL, in 100 mmol/L of phosphate, at pH 7.0, 50 mmol/L of NaCl, after heating at 323, 333 and 343 K, followed by cooling back to 298 K and removal of precipitate (see Section 2.4 for details). Insert corresponds to 343 K data. Data acquisition absorbance at 414 nm.

precipitation/aggregates at both temperatures, 323 and 333 K, is not observed as noticed in the centrifugation step, prior to AUC analysis. At 343 K, the oxy-HbGp undergoes complete oligomeric dissociation into smaller subunits, and the monomer ***d*** and trimer ***abc*** subunits are observed in the c(S) distribution (see the insert of Fig. 3, circles). The $s^0_{20,w}$ and *MM* values are 1.8 ± 0.1 S, 17.7 ± 0.1 kDa for the monomer ***d***, and 3.5 ± 0.2 S, and 51.3 ± 0.6 kDa, for the trimer ***abc*** (insert in Fig. 3 and Table 2). The *MM* and $s^0_{20,w}$ values for the monomer ***d*** and trimer ***abc*** are quite similar to previous HbGp studies, at alkaline pH [25]. The relative percentages in the solutions used for AUC were 70 ± 5% for the monomer and 30 ± 2% for the trimer subunits. The smaller contribution of the trimer as compared to the monomer can be, probably, explained as due to the low stability of the isolated trimeric subunit in the solution. Thus, the observed precipitate formed in the solution, at 343 K, is, probably, associated to the partial precipitation of the trimer (***abc***), as observed in previous studies of isolated HbGp subunits [7].

Thus, our present AUC complimentary data show, clearly, that HbGp maintains, to a significant extent, its undissociated structure, at the temperature of 323 K. Moreover, HbGp undergoes oligomeric dissociation and denaturation, at the temperatures of 333 and 343 K, in agreement with the DSC results that report an irreversible denaturation process for oxy-HbGp.

3.3. Thermal aggregation of HbGp studied by dynamic light scattering

The DLS data are quite informative since they allow monitoring the hydrodynamic diameter (D_h) and the light scattering intensity (intensity in counts/s) of particle formed in solution, in the course of the protein thermal aggregation, as well as, to obtain the kinetic parameters. The size distribution curves of the particles measured at different times of incubation of oxy-HbGp, at 1.0 mg/mL, and 323 K, are shown in Fig. 4. In the initial time (t = 0 min) the size distribution of the particles presents a single sharp peak, associated to the native protein, with D_h of 27 nm [13–15]. The system remains monodisperse for a long time of incubation (228 min-almost 4 h, Fig. 4), with the appearance of a second peak at 228 min, as indicated by the arrow (Fig. 4). This peak is attributed to the protein aggregation and it becomes more pronounced with time, as can be observed in the curves for incubation times of 261 and 294 min. Moreover, the aggregates contribute equally to the main peak for native HbGp at 294 min, becoming predominant at longer times, as shown for the plot at 549 min. At 600 min of incubation, the HbGp is completely aggregated (Fig. 4). The increase of temperature leads to the appearance of aggregation in solution at an earlier time, and, the complete HbGp aggregation is achieved also at shorter times. The size distribution curves for the thermal aggregation of HbGp, at 0.5 and 3.0 mg/mL, are similar to those shown in Fig. 4.

The increase of HbGp concentration leads to the increase in the time required for aggregation. The increase of temperature also promotes the formation of aggregates earlier (data not shown). For example, at HbGp concentration of 3.0 mg/mL, a smaller time of incubation is required for the onset of the second peak (213 min), and an equal contribution of aggregates and native protein occurs

Table 2
Hydrodynamic properties for the oxy-HbGp at pH 7.0, heated at indicated temperatures (left column) for 1 h, cooled back to 298 K, centrifuged to remove precipitate, and analyzed at 298 K, by sedimentation velocity (SV) ultracentrifugation.

Temperature (K)	Species	Hydrodynamic properties		
		$s^0_{20,w}$ (S)[a]	*MM* (kDa)[b]	Area (%)[c]
323	Whole HbGp	57 ± 1	3530 ± 50	100
333	Tetramer ***abcd***	4.2 ± 0.3	67.1 ± 0.2	12 ± 3
	Whole HbGp	56 ± 1	3430 ± 80	88 ± 5
343	Monomer ***d***	1.8 ± 0.1	17.7 ± 0.1	70 ± 5
	Trimer ***abc***	3.5 ± 0.2	51.3 ± 0.6	30 ± 2

[a] Data obtained from linear regression.
[b] Molecular masses (*MM*) estimated by the SEDPHAT software using global fitting.
[c] Percentage of HbGp species, based on the area in the c(S) distributions, obtained from SEDFIT software.

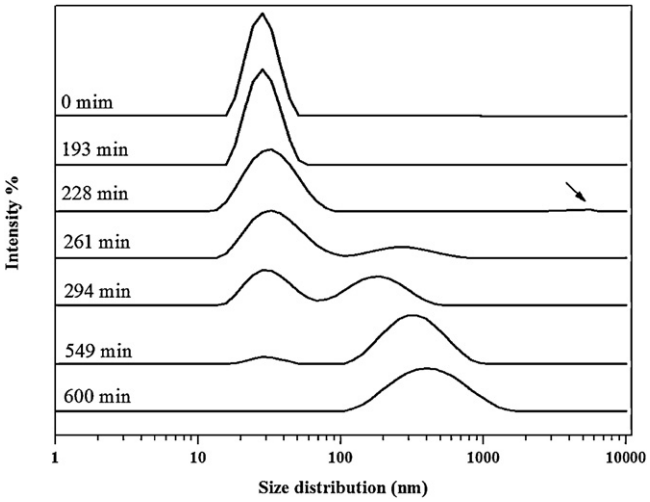

Fig. 4. Size distributions vs intensity (%) plots for oxy-HbGp, at 1.0 mg/mL, in phosphate buffer 30 mmol/L, at pH 7.0, 323 K, and indicated times of incubation. The arrow at 228 min indicates the start of aggregates appearance in solution.

after 327 min; the appearance of aggregates only takes place at 1034 min (data not shown). However, for HbGp concentration of 0.5 mg/mL, at 323 K, the time of incubation required for the appearance of aggregates in solution is considerably larger (261 min). An equal contribution in the size distribution of aggregate and native protein occurs at 309 min, with predominance of aggregates at 534 min (data not shown).

In Fig. 5 the D_h (nm) and scattering intensity (counts/s) plots are shown for oxy-HbGp, at concentrations of 1.0 (Fig. 5A and B) and 3.0 (Fig. 5C and D) mg/mL, in the temperature range from 323 to 327 K, respectively. The analysis of the curves using Eq. (1) allowed obtaining the lag period for different temperatures and HbGp concentrations (Table 3 and insert of Fig. 5A). These data show a lag period of 193 min for HbGp, at 1.0 mg/mL, incubated at 323 K (Fig. 5A).

Table 3 shows that, independent of the protein concentration and temperature value, the minimum size of the aggregate, $D_{h,0}$, corresponds to the native HbGp hydrodynamic diameter of 27.5 nm [13,15]. This means that the native, oligomeric HbGp, has an appropriate dimension to produce larger aggregates, differently from the smaller proteins reported in the literature that require the nucleation of a minimum size complex for aggregation to start [20,28,31,34]. Concerning the lag time t_0, it increases significantly on going from 0.5 to 1.0 mg/mL of protein, from 112 to 193 min. The explanation for its decrease, on further increase of protein concentration to 3.0 mg/mL (175 min), is the fact that at higher protein concentration the aggregation process starts earlier.

Another interesting parameter also shown in Table 3 is t_{2D}, associated to the reciprocal of HbGp aggregation rate. t_{2D} becomes higher with the increase of protein concentration at 323 K (Table 3). Moreover, it has a significant decrease with increase of temperature, in the three protein concentrations, indicating that the aggregation process becomes faster. This higher t_{2D} value of 197 min observed for the HbGp concentration of 0.5 mg/mL, at 327 K, may be attributed to the formation of the oxidized species such as, aquo-met-HbGp and hemichrome, as will be shown later in this paper (spectroscopy section).

The differences in the parameters lag period (t_0), t_{2D} and on the time required for the formation of the first aggregates observed for HbGp, in the concentration range from 0.5 to 3.0 mg/mL, at 323 K, can be explained in the following way: as can be observed in Fig. 5B and D, HbGp undergoes oligomeric dissociation before aggregation, noticed by the reduction in the counting rate at initial times. Moreover, the increase of HbGp concentration from 1.0 to 3.0 mg/mL makes the oligomeric dissociation process shorter, with the aggregates formation in solution slightly earlier (Fig. 5B and D). For HbGp concentration of 0.5 mg/mL the oligomeric dissociation is less pronounced and the increase of the D_h (nm) occurs in a shorter time. However, the lower HbGp concentration (0.5 mg/mL) requires a larger time for the formation of the first aggregates in solution. In Fig. 5B and D the precipitation of the aggregates is also clear after 574 min (for 1.0 mg/mL) and 578 min (for 3.0 mg/mL), at 323 K, as evidenced by an abrupt decrease on the scattering intensity.

Thus, our DLS kinetic data show clearly that the protein concentration is a very important factor on the thermal aggregation of HbGp. Our present results are in agreement with previous studies [15]. More detailed investigations on the aggregation process of HbGp will be a very interesting matter for future research.

3.4. Optical absorption studies for oxy- and cyanomet-HbGp

Fig. 6A shows the optical absorption spectra of oxy-HbGp, at pH 7.0, as a function of the temperature, in the range from 293 to 343 K. These absorption spectra show the characteristic bands of hemoproteins, namely, the intense Soret band centered at 415 nm for oxy- and at 420 nm for cyanomet-HbGp (not shown), the Q-bands in the 480–600 nm range (see in Fig. S2, the expanded Q-bands), and the band for aromatic amino acids centered at 280 nm. The cyanomet-HbGp has a single broad Q-band centered at 540 nm (see Fig. S2B), while the oxy-form has the characteristic two bands centered at 540 and 575 nm (see Fig. S2A). The increase in the temperature leads to a decrease in the oxy-HbGp Soret band intensity, with a simultaneous blue-shift from 415 to 405 nm, as indicated by arrows in Fig. 6A. Fig. 6B and C shows that the oxy-HbGp, at pH 7.0 is stable up to 325 K, showing a decrease in the absorbances at 415 nm and Q-bands (see also Fig. S2A), at higher temperatures. The cyanomet-HbGp, at pH 7.0, has a similar stability compared to the oxy-form (Fig. 6C). Figs. S2A and S2B show clearly that above 327 K, dramatic changes occur in the Q-bands for both oxy- and cyanomet-HbGp, consistent with the presence in solution of a mixture of species, probably, met-HbGp and hemichrome. Moreover, the increase in the intensity of the 630 nm band (see Fig. S3) gives evidence that a high-spin heme protein species is formed in solution [27,35,36].

Plots of the experimental data together with the corresponding fits, based on the two-state model given in Eq. (2), using the Soret band absorbances, at 415 nm for oxy- and 420 nm for cyanomet-HbGp, at pH 7.0, are shown in Fig. 6C. The absorbance plots, for both HbGp oxidation forms, show clearly small changes in the lower temperature range, between 292 and 325 K. These gradual changes of slopes may be associated to the iron oxidation and structural changes induced by temperature. Since HbGp is an oligomeric protein, it could initially, at lower temperatures, undergo conformational changes and partial oligomeric dissociation upon heating; the denaturation and unfolding processes would take place subsequently, at higher temperatures, as a second step in the global transition. Such interpretation could explain the slope, observed in the low temperature range for the curves shown in Fig. 6C.

Moreover, the fits based on the two-state model allowed to obtain the critical temperature, T_c, associated to the thermal denaturation process. The apparent enthalpy values, ΔH_{app}, obtained from these fits, are not discussed here since the HbGp thermal denaturation involves the onset of an aggregation process, as shown by DLS data in Section 3.3. For oxy- and cyanomet-HbGp T_c values of 331 ± 2 K and of 332 ± 2 K, respectively, were obtained (Fig. 6C and Table 4). Although, a slightly higher dependence with temperature for cyanomet-HbGp, as compared to the oxy-form, is observed (higher slope, Fig. 6C), the differences of the T_c values are not significant (Table 4). Our previous studies of HbGp thermal

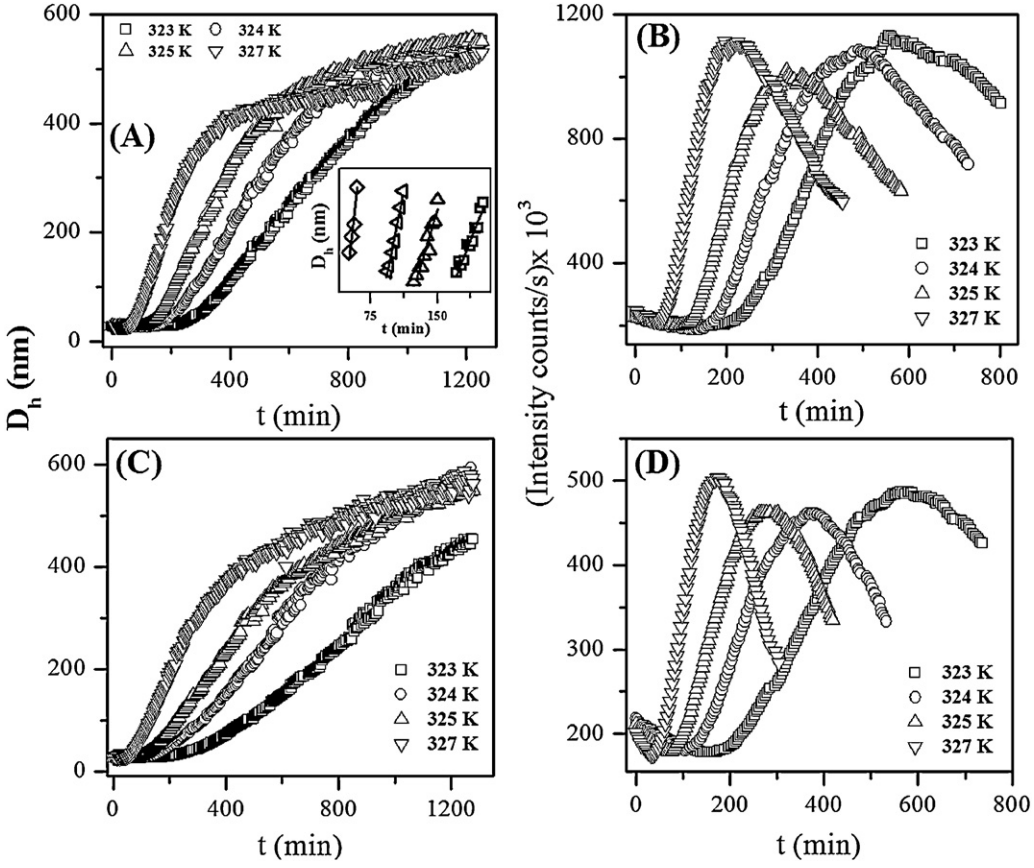

Fig. 5. Thermal aggregation kinetic plots for oxy-HbGp, at pH 7.0, in phosphate buffer 30 mmol/L, and indicated temperatures. Protein concentrations are 1.0 mg/mL (A) and (B) and 3.0 mg/mL (C) and (D). The hydrodynamic diameter, D_h (in nm, A and C), and scattering intensity (in counts/s, B and D) are shown, respectively, in the left and right panels. Insert in (A) corresponds to the fits obtained based on the Eq. (1) (see Section 2.3).

denaturation, based on DLS [13,14], did not revealed this temperature dependence at lower temperatures. In fact, the size of the scattering particles (protein molecules) remains constant up to the critical temperatures [13]. This is related to the fact that DLS technique detects global changes of the particle as a whole, while optical absorption of the heme group transitions reports on the local environment of the metal in the macrocycle, being more sensitive to local changes induced by the temperature. T_c values obtained using optical absorption spectroscopy are very similar to the values obtained by the other techniques [13,14].

The difference on the thermal stability of oxy-HbGp, in acidic and neutral media, is quite well evidenced in Fig. 6B: temperatures higher than 331 K (pH 5.0) and 333 K (pH 6.0) induce, a strong aggregation process for oxy-HbGp, followed by an intense light scattering (see the points with higher "absorbances" in Fig. 6B). For this reason, the high temperature absorbance data, for acidic pH, were omitted in Fig. 6B. On the other hand, in neutral pH 7.0, HbGp undergoes denaturation and the formation of aggregates in solution is not observed (Fig. 6B). Thus, our absorption data show that, the increase of pH values in the order pH 5.0 > pH 6.0 > pH 7.0, disfavors the thermal aggregation process. Our present results are consistent with previous observations, based on dynamic light scattering, where HbGp forms large aggregates in acidic media and high temperature [13,14].

Table 3
Parameters obtained from the dependence of the hydrodynamic diameter, D_h, on time, for the oxy-HbGp aggregation, at pH 7.0, and indicated temperatures and protein concentrations.

[oxy-HbGp] (mg/mL)	Temperature (K)	$D_{h,0}$ (nm)	t_0 (min)	t_{2D} (min)
0.5	323	27.6 ± 0.1	112 ± 1	29 ± 1
	324	27.4 ± 0.2	73 ± 1	22 ± 1
	325	27.3 ± 0.1	30 ± 1	17 ± 1
	327	27.4 ± 0.2	50 ± 1	197 ± 33
1.0	323	27.7 ± 0.1	193 ± 1	611 ± 70
	324	27.6 ± 0.2	148 ± 1	273 ± 15
	325	27.5 ± 0.1	108 ± 1	149 ± 8
	327	27.8 ± 0.3	56 ± 1	137 ± 9
3.0	323	27.4 ± 0.1	175 ± 1	448 ± 20
	324	27.4 ± 0.1	118 ± 1	300 ± 10
	325	27.4 ± 0.2	82 ± 1	240 ± 2
	327	27.2 ± 0.3	42 ± 1	198 ± 20

The parameters $D_{h,0}$, t_0, and t_{2D} were obtained from fits to Eq. (1) [20]. Based on DLS data (see Fig. 5).

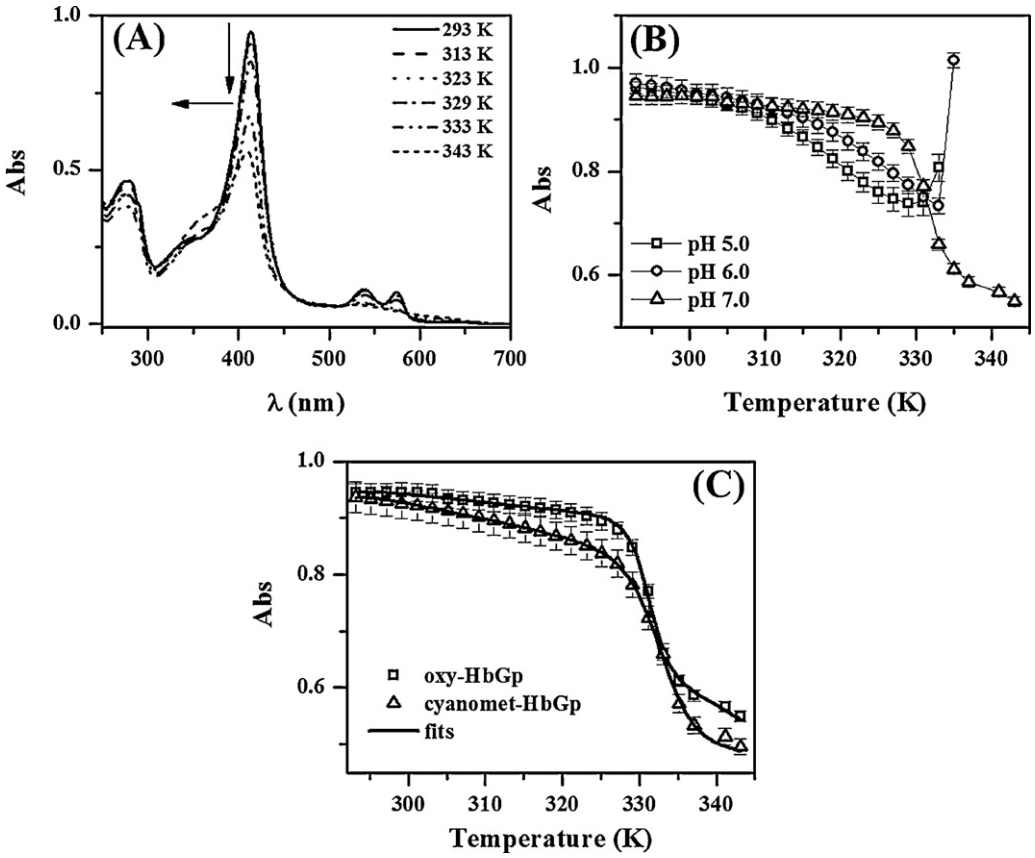

Fig. 6. (A) Optical absorption spectra for oxy-HbGp 0.2 mg/mL, in acetate–phosphate buffer 30 mmol/L, at pH 7.0, in the temperature range from 293 to 343 K. The arrows indicate the direction of absorbance changes with temperature increase. (B) Soret band absorbance, at 415 nm, for oxy-HbGp, at indicated pH values from 5.0 to 7.0. (C) Absorbance for oxy- (415 nm) and cyanomet-HbGp (420 nm), at pH 7.0. The symbols correspond to the experimental values and the full lines to the fits by Eq. (2) [19].

3.5. CD thermal stability studies for oxy- and cyanomet-HbGp

Oxy-HbGp CD spectra show a local minimum at 222 nm, typical of α-helical structure, and a band at 195 nm, associated to the peptide bonds (Fig. 7A). In the UV-VIS range, peaks corresponding to the Soret band at 415 nm, for oxy-HbGp (Fig. 7B), and 420 nm for cyanomet-HbGp (data not shown), characteristic of heme asymmetry, and also aromatic amino acid peaks, centered around 260–262 nm, for both oxidation forms, are observed [26].

Based on the spectra shown in Fig. 7A (see also Fig. 7C), oxy-HbGp is stable, at pH 7.0, with minor ellipticity changes, in the range from 293 to 323 K. A significant decrease of ellipticity intensity is observed only above 325 K (Fig. 7C). At pH 5.0, the behavior is quite similar to that at pH 7.0. The observed ellipticity value does not reach zero at 353 K, suggesting that the HbGp denaturation process is not complete. In acidic pH, the ellipticity monitored at 222 nm, and 353 K, is smaller as compared to the neutral solution. This is, probably, due to the sedimentation of the aggregates formed at high temperatures, while at pH 7.0 no protein precipitation is observed.

In Fig. 7C the HbGp ellipticity plots, at 222 nm, are shown, as a function of temperature, together with the two-state model fits (Eq. (2)). Both HbGp oxidation forms undergo an irreversible thermal denaturation process, as monitored in the peptide and heme group (data not shown) regions. The HbGp transition from the folded to the unfolded states is very fast, especially in acidic pH values of 5.0 and 6.0, remaining a small protein fraction in solution (low ellipticity, Fig. 7C). This observation is, probably, an indication that protein aggregation is an important step on the HbGp thermal denaturation, in the two oxidation forms, being dependent on the pH value.

Besides, the temperature induces a shift in the Soret band wavelength maximum from 415 nm to 435 nm (see Fig. 7B), which could

Table 4
Critical temperatures (T_c) for HbGp, in the oxy- and cyanomet-forms, based on the optical absorption (415 and 420 nm), and CD peptide bonds (222 nm) and heme group (415 and 420 nm) regions, at indicated pH values.

	pH	$Abs_{415\,nm}$	$CD_{222\,nm}$	$CD_{415\,nm}$
Oxy-HbGp	5.0	–	335 ± 2	–
	6.0	–	336 ± 1	338 ± 2
	7.0	331 ± 2	329 ± 2	334 ± 3
	pH	$Abs_{420\,nm}$	$CD_{222\,nm}$	$CD_{420\,nm}$
Cyanomet-HbGp	5.0	–	337 ± 1	336 ± 3
	6.0	–	339 ± 2	341 ± 4
	7.0	332 ± 2	333 ± 2	337 ± 3

T_c was obtained by fits based on the two state model (Eq. (2)) [19].

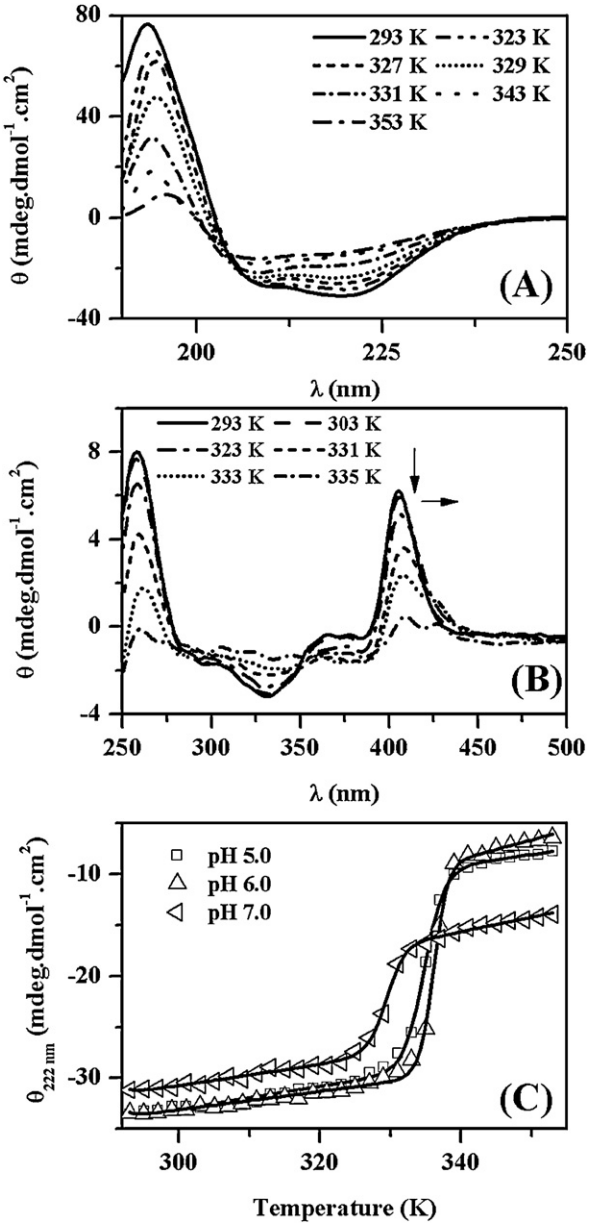

Fig. 7. CD spectra for oxy-HbGp, in acetate–phosphate buffer 30 mmol/L, pH 7.0, in the temperature range from 293 to 353 K. (A) Peptide bonds region, at 0.2 mg/mL protein, and (B) heme group and aromatic amino-acids region, at 3.0 mg/mL. (C) Molar ellipticity at 222 nm, for oxy-HbGp, as a function of temperature, in the indicated pH values from 5.0 to 7.0, fitted with the two-state model. Symbols correspond to the experimental values and full lines to the fits by Eq. (2) [19].

be due to the formation of some HbGp oxidized form. This spectral change occurs above 323 K, remaining as such in the temperature range from 318 to 333 K, and being, probably, associated to a hemichrome formation, as a result of oxy-HbGp oxidation, in agreement with optical absorption results. Thus, it is possible that the oxy-HbGp oxidation, together with the unfolding process, leads to the exposure of the heme groups to the solvent, allowing the access of water molecules to the heme pocket, shifting the Soret band CD signal (Fig. 7B) through changes in the iron coordination [11].

The fittings of the experimental data shown in Fig. 7C allowed to obtain the T_c values in the pH range from 5.0 to 7.0, associated with HbGp denaturation. For cyanomet-HbGp, the ellipticity plots are similar to those obtained for oxy-HbGp (Fig. 7C), presenting a slight shift to higher temperatures, and giving adequate fits based on the two-state model (not shown). In the heme group region, at 415 nm (Soret band), for oxy-HbGp, the plots are similar to those obtained at 222 nm, with a slightly higher T_c (Table 4). All T_c values obtained from CD data analysis are collected in Table 4. They show that oxy- and cyanomet-HbGp present a similar T_c, in agreement with optical absorption results.

At pH 5.0, a reasonable fit was not achieved, since a different profile was observed (see Fig. S4A), associated to the formation of another species upon thermal denaturation, due to the auto-oxidation of the heme group iron with increase of the temperature. A small shift of the Soret band wavelength to higher value is observed, together with an increase in intensity (Fig. S4). These spectral changes can be due to the heme group asymmetry variations, probably, associated to the iron auto-oxidation induced by the high temperature. These changes were not observed for the aromatic amino-acids band, monitored at 260 nm (not shown).

4. Conclusions

DSC studies show that the HbGp, at pH 7.0, has a thermal denaturation process partially reversible, dependent on the heating temperature. Furthermore, when the HbGp is heated up to a critical temperature a fully irreversible denaturation takes place. DSC data show systematically higher T_c values for cyanomet-HbGp as compared with those obtained for oxy-HbGp supporting a higher stability of the oxidized form, at acidic and neutral pH. Both HbGp oxidation forms present endotherms composed of, at least, two components in acidic media. At pH 7.0, oxy-HbGp presents a very cooperative single component thermogram, while for cyanomet-HbGp two components are observed, implying the existence of an intermediate state in acidic medium, as monitored by global denaturation. In addition, AUC data show that HbGp maintains its undissociated structure, at 323 K, presenting an increase in oligomeric dissociation at higher temperatures of 333 and 343 K. The thermal aggregation studies by DLS show, for the first time, a lag time (t_0) dependent on the temperature and HbGp concentration. The oligomeric dissociation of HbGp before the aggregation process is noticed, being more pronounced at concentrations 1.0 and 3.0 mg/mL, since, at the lower protein concentration, the dissociation and aggregation significantly overlap. Both HbGp forms seem to form oxidized species such as hemicrome and aquo-met-HbGp, at high temperatures. They have very similar T_c values, as monitored by CD and optical absorption. All present results on the HbGp thermal denaturation and aggregation are consistent with previous studies of HbGp thermal stability by DLS and DSC.

Acknowledgements

The authors are indebted to Mr. Ézer Biazin (Instituto de Química de São Carlos, Universidade de São Paulo) for excellent technical assistance with HbGp sample preparations. Thanks are due to Dr. Fernando Melo for help at the initial stage of our DSC work, and to Mrs. Andressa Patrícia Alves Pinto (Instituto de Física de São Carlos, Universidade de São Paulo) for help with the calorimetric experiments. Thanks are due to the Spectroscopy and Calorimetry Laboratory of the National Biosciences Laboratory (LNBio, Campinas, Brazil) and National Synchrotron Light Laboratory (LNLS, Campinas, Brazil) for making available the instrumentation used for the DSC and AUC experiments reported in this work. Thanks are due to the Brazilian agencies FAPESP, CNPq, and CAPES for partial financial support. F.A.O. Carvalho is a recipient of a Ph.D. grant from FAPESP (2009/17261-6). J.W.P. Carvalho is a recipient of a Ph.D. grant from FAPESP (2010/09719-0). M. Tabak is grateful to CNPq for a research grant.

Appendix A. Supplementary data

Supplementary data associated with this article can be found, in the online version, at http://dx.doi.org/10.1016/j.ijbiomac.2012.11.022.

References

[1] S.N. Vinogradov, Micron 35 (2004) 127–129.
[2] F. Zal, B.N. Green, P. Martineu, F.H. Lallier, A. Toulmond, S.N. Vinogradov, J.J. Childress, European Journal of Biochemistry 267 (2000) 5227–5236.
[3] A. Krebs, P. Zipper, S.N. Vinogradov, Biochimica et Biophysica Acta 1297 (1996) 115–118.
[4] W.E. Royer Jr., H. Sharma, K. Strand, J.E. Knapp, B. Bhyravbhatla, Structure 14 (2006) 1167–1177.
[5] F.A.O. Carvalho, P.S. Santiago, J.C. Borges, M. Tabak, Analytical Biochemistry 385 (2008) 257–263.
[6] M.S. Oliveira, L.M. Moreira, M. Tabak, International Journal of Biological Macromolecules 40 (2007) 429–436.
[7] F.A.O. Carvalho, J.W.P. Carvalho, P.S. Santiago, M. Tabak, Process Biochemistry 46 (2011) 2144–2151.
[8] M. Rousselot, E. Delpy, C.D. La Rochelle, V. Lagente, R. Pirow, J. Rees, A. Hagege, D. Lee Guen, S. Hourdez, F. Zal, Biotechnology Journal 1 (2006) 333–345.
[9] P.D. Martin, A.R. Kuchumov, B.N. Green, R.W. Oliver, E.H. Braswell, J.S. Wall, S.N. Vinogradov, Journal of Molecular Biology 255 (1996) 154–169.
[10] A.L. Poli, L.M. Moreira, M. Tabak, H. Imasato, Colloids and Surfaces B 52 (2006) 96–104.
[11] S.C.M. Agustinho, M. Tinto, J.S. Perussi, M. Tabak, H. Imasato, Comparative Biochemistry and Physiology 118A (1998) 171–181.
[12] J.F.R. Bachega, L. Bleicher, E.R. Horjales, P.S. Santiago, R.C. Garratt, M. Tabak, Journal of Synchrotron Radiation 18 (2011) 24–28.
[13] P.S. Santiago, F. Moura, M.L. Moreira, M.M. Dominguis, N. Santos, M. Tabak, Biophysical Journal 94 (2008) 2228–2240.
[14] P.S. Santiago, F.A.O. Carvalho, M.M. Domingues, J.W.P. Carvalho, N.C. Santos, M. Tabak, Langmuir 26 (12) (2010) 9794–9801.
[15] P.S. Santiago, J.W.P. Carvalho, M.M. Domingues, N.C. Santos, M. Tabak, Biophysical Chemistry 152 (1–3) (2010) 128–138.
[16] J.M. Sanchez-Ruiz, Biophysical Journal 61 (1992) 921–935.
[17] E. Freire, K.P. Murphy, J.M. Sanchez-Ruiz, M.L. Galisteo, P. Privalov, Biochemistry 31 (1992) 250–256.
[18] C.E. Dempsey, T.J. Piggot, P.E. Mason, Biochemistry 44 (2005) 775–781.
[19] L.A. Campos, J. Sancho, Proteins 63 (2006) 581–594.
[20] K.A. Markossian, H.A. Khanova, S.Y. Kleimenov, D.I. Levistsky, N.A. Chebotareva, R.A. Asryants, V.I. Muronetz, L. Saso, I.K. Yudin, B.I. Kurganov, Biochemistry 45 (2006) 13375–13384.
[21] J. Lebowitz, M.S. Lewis, P. Schuck, Protein Science 11 (2002) 2067–2079.
[22] P. Schuck, Biophysical Journal 78 (2000) 1606–1619.
[23] P. Schuck, M.A. Perugini, N.R. Gonzales, G.J. Howlett, D. Schubert, Biophysical Journal 82 (2002) 1096–1111.
[24] P. Schuck, Analytical Biochemistry 320 (2003) 104–124.
[25] F.A.O. Carvalho, P.S. Santiago, J.C. Borges, M. Tabak, International Journal of Biological Macromolecules 48 (2011) 183–193.
[26] S.M. Kelly, J.J. Thomas, N.C. Price, Biochimica et Biophysica Acta 1338 (1997) 161–185.
[27] F.A.O. Carvalho, P.S. Santiago, M. Tabak, Archives of Biochemistry and Biophysics 519 (2012) 46–58.
[28] A.E. Lyubarev, B.I. Kurganov, A.A. Burlakova, V.N. Orlov, Biophysical Chemistry 70 (1998) 247–257.
[29] K. Idakieva, N.I. Siddiqui, K. Parvanova, P. Nikolov, C. Gielens, Biochimica et Biophysica Acta 1764 (2006) 807–814.
[30] K. Idakieva, C. Gielens, N.I. Siddiqui, L. Doumanova, B. Vasseva, G. Kostov, V.L. Shnyrov, Zeitschrift für Naturforschung A 62a (2007) 499–506.
[31] K. Idakieva, P. Nikolov, I. Chakarska, N. Genov, V.L. Shnyrov, Journal of Fluorescence 18 (2008) 715–725.
[32] K. Idakieva, K. Parvanova, S. Todinova, Biochimica et Biophysica Acta 1748 (2005) 50–56.
[33] L. Bao, S. Chatterjee, S. Lohmer, D. Schomburg, Protein Journal 26 (2007) 143–151.
[34] I. Quesada-Soriano, F. García-Maroto, L. García-Fuentes, Biochimica et Biophysica Acta 1764 (2006) 979–984.
[35] E. Droghetti, S. Sumithran, M. Sono, M. Antalík, M. Fedurco, J.H. Dawson, Archives of Biochemistry and Biophysics 489 (2009) 68–75.
[36] M.S. Hargrove, J.S. Alson, Biochemistry 35 (1996) 11310–11318.